Photochemical & Photobiological Sciences

RSC Publishing

PAPER

View Article Online
View Journal

Cite this: DOI: 10.1039/c3pp25410k

Nonlinear absorption properties of 5,10-A_2B_2 porphyrins – correlation of molecular structure with the nonlinear responses

Monika Zawadzka,[a] Jun Wang,[b] Werner J. Blau[c] and Mathias O. Senge*[a]

The nonlinear absorption properties of two series of novel free base and metalated *meso* 5,10-A_2B_2 substituted porphyrins, both bearing *p*-tolyl as an A substituent and TMS-ethynyl or bromine as a B substituent, were investigated with the open Z-scan technique at 532 nm in the ns time regime. Most of the compounds exhibited a transmission drop with increasing input fluence. This behavior is desirable for their applications in optical limiting. More complex responses: a drop in transmission followed by an increase in transmission or an increase in transmission followed by a transmission drop, with increasing input fluence, were detected for certain compounds. All of the recorded responses were successfully fitted with a four-level model with simultaneous two-photon absorption arising from the higher excited states (consecutive one- + one- + two-photon absorption). The TMS-ethynyl group was found to be a more efficient *meso* substituent in optical limiting than the bromine atom. Indium, lead and zinc complexes with TMS-ethynyl substituents were the strongest positive nonlinear absorbers amongst compounds studied which makes them the most interesting candidates for optical limiting application.

Received 2nd December 2012,
Accepted 8th March 2013

DOI: 10.1039/c3pp25410k

www.rsc.org/pps

Introduction

The development of new materials with enhanced nonlinear optical (NLO) responses is of great scientific interest.[1,2] Porphyrins, along with phthalocyanines and other related macrocyclic dyes, constitute a promising group of NLO compounds due to high nonlinearities upon irradiation with high intense laser light.[3,4] Their main advantage is their chemical versatility which provides a tool for tailoring the linear and NLO properties for specific applications. One field of potential use of NLO active macrocyclic dyes is broadband optical limiting (OL), which aims for the protection of human eyes and sensitive optical elements against accidental exposure to high energy laser beams.[5] An optical limiter remains transparent to low fluence light and becomes opaque at high light fluence.

Macrocyclic dyes are characterized by a linear absorption spectral window in the visible range. Within that range positive nonlinear absorption (NLA) giving rise to an OL effect was reported for compounds with various structures.[6] Such a response arises from sequential absorption of photons and is referred to as reverse saturable absorption (RSA). RSA occurs if the absorption arising from the excited states is higher than that arising from the ground state. Otherwise, the opposite effect, *i.e.* saturable absorption (SA), takes place. The contribution of specific excited states to NLA depends on pulse duration and applied intensities. At higher inputs higher excited states can be populated and hence have an impact on NLA, at lower inputs it is usually satisfactory to consider only first singlet and/or triplet excited states when modeling the NLA response. Under subnanosecond pulses the contribution of triplet states can usually be neglected, as intersystem crossing (ISC) is on the order of nanoseconds. Under nanosecond or longer pulses triplet states become populated. The effective generation and rapid access to triplet states are of great interest for protection against longer pulses as the triplet states are long lived (lifetime on the order of microseconds) and therefore will not decay within pulse duration. Hence, candidates for OL application should exhibit a high quantum yield for triplet state formation, rapid ISC and a high ratio of the excited state absorption cross-section to that of the ground state. Additionally, they should have narrow linear absorption features to ensure high transmission at high concentration and absorb nonlinearly high fluence light over a broad wavelength range. Good thermal- and photo-stability and ease of processability are desirable as well.[7] Relevant research in this area focuses on the synthesis of new compounds,[8] materials composition,[9] and a better understanding of complex NLO responses.[7,10]

Significant progress has been made in the improvement of the OL performance of porphyrins since the first observation

[a]*School of Chemistry, SFI Tetrapyrrole Laboratory, Trinity Biomedical Sciences Institute, Trinity College Dublin, Dublin 2, Ireland. E-mail: sengem@tcd.ie; Fax: +353 1 896 8536; Tel: +353 1 896 8537*
[b]*Key Laboratory of Materials for High Power Lasers, Shanghai Institute of Optics and Fine Mechanics, Chinese Academy of Science, 201800 Shanghai, China*
[c]*School of Physics, Trinity College Dublin, Dublin 2, Ireland*

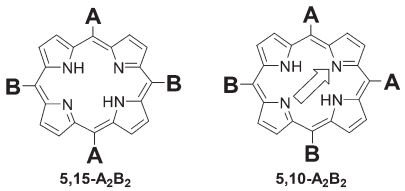

Fig. 1 Molecular formula of 5,15- and 5,10-A_2B_2-type porphyrins.

of the OL effect in TPP in 1985.[5,11,12] Most studies focused on highly symmetric *meso* tetrasubstituted compounds and a few reports on *meso* and β-substituted compounds or 5,15-A_2B_2-type porphyrins have been published.[13,14] Most studies investigated either substituent or central metal effects on the OL performance. Still, consistent structure–OL performance relationships are not yet in hand. The presence of a central metal atom was demonstrated in many reports to improve NLA *via* enhancement of the ISC rate and the quantum yield for triplet states due to the heavy atom effect. Likewise, the incorporation of conjugated groups at the *meso* positions was shown to enhance the OL action of porphyrins. (5,10,15,20-Tetra(trimethylsilylethynyl)porphyrinato)lead(II)[7] and lead, indium and thallium complexes of 5,10,15,20-tetra(triisopropylsilylethynyl)porphyrin[15] provided the best OL porphyrins up to date. The highest ratio of the excited to the ground state absorption cross-section reached values in the range of 45–48. Moreover, other reports explored other means of OL response tuning through incorporation of different axial ligands,[16] protonation of free base compounds,[17] oligomerization of porphyrins,[18] or binding of porphyrins to other OL materials such as graphene or fullerene.[19] Generally speaking NLA is very susceptible to structural modifications of the basic dyes potentially allowing further progress in the OL field.

Recently we reported on the synthesis of a relatively unexplored class of porphyrins, the 5,10-A_2B_2-type systems (Fig. 1).[20] Their different alignment of the intramolecular dipole moment makes them an interesting class of potential dyes. Previous research on such porphyrins carried out by us revealed an interesting, though undesirable for OL application, behavior upon irradiation with high fluence light, *i.e.* a RSA/SA switch.[21] A continuation of these studies elucidated further interesting NLA responses (*e.g.*, RSA/RSA, SA/RSA/SA, RSA/SA) along with the typically observed RSA.[22] Clearly further studies were warranted and here we focus on the comparative analysis of two series of 5,10-A_2B_2 porphyrins. We show these systems to be interesting candidates for OL application upon certain structural modifications and highlight the interesting and diverse NLA responses of 5,10-A_2B_2-type porphyrins, which depend on structural features such as the central metal and the type of *meso* substituent.

Results and discussion

Synthesis

Based on previous studies in which we identified {5,15-bis-(3-methoxyphenyl)-10,20-di[(trimethylsilyl)ethynyl]porphyrinato}-zinc(II) as the most promising among numerous porphyrins with varied *meso* substituents[14] and the literature indicated the utility of lead porphyrins with (trimethylsilyl)ethynyl (TMS-ethynyl) groups,[7] thus, we decided to further explore the potential of the very promising TMS-ethynyl substituent in the context of 5,10-A_2B_2 porphyrins.

The synthesis of such compounds started with porphyrin **H_2_Br** which was synthesized following a procedure reported before.[20] The general chemical route adapted for the synthesis of two series of such compounds is shown in Scheme 1. Metalation[23] of compound **H_2_Br** with different metal salts ($InCl_3$, $Pd(acac)_2$, $PtCl_2$, $Pb(acac)_2$, $Zn(acac)_2$ and $SnCl_2$) gave the brominated metal complexes: **InCl_Br**, **Pd_Br**, **Pt_Br**, **Pb_Br**,

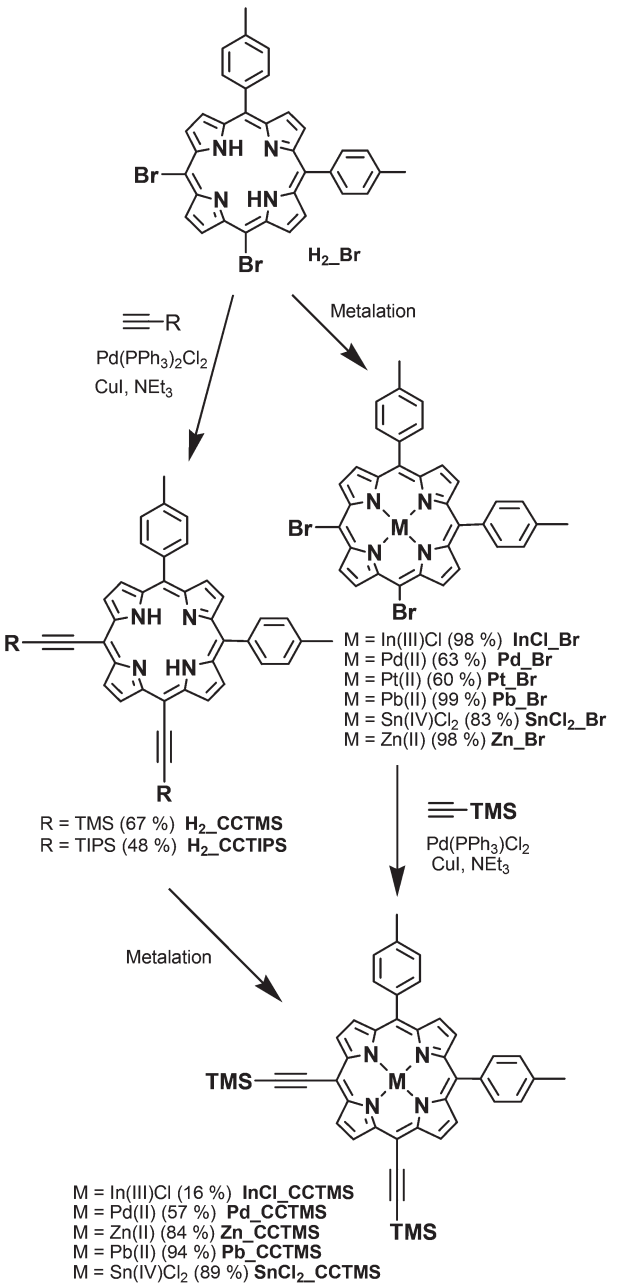

Scheme 1 Synthesis of 5,10-A_2B_2-porphyrins.

Zn_Br and **$SnCl_2$_Br**, respectively. The free base and metalated porphyrins **H_2_Br**, **InCl_Br**, **Pd_Br** and **Zn_Br** were then subjected to Sonogashira coupling[24] with TMS-acetylene to provide the compounds **H_2_CCTMS**, **InCl_CCTMS**, **Pd_CCTMS** and **Zn_CCTMS**, respectively. Similar coupling reactions of **H_2_Br** with TIPS-acetylene provided compound **H_2_CCTIPS**.

Sonogashira coupling could be achieved with the lead complexes as well. However, during the chromatographic work-up complete demetalation was observed. Such low stability of Pb(II) complexes has been noted before.[25] Thus, the direct metalation of compound **H_2_CCTMS** to **Pb_CCTMS** was used for the preparation of this complex. A similar procedure was used for the preparation of the tin(IV) complex **$SnCl_2$_CCTMS**. A platinum complex with TMS-ethynyl substituents could not be obtained following either route.

Characterization

Mass spectrometry (MS) enabled the unambiguous identification of the chloride axial ligands in Sn(IV) and In(III) complexes. Peaks in agreement with the calculated isotopic patterns were observed in the region corresponding to the molecular ion [M] and [M − Cl] for **InCl_Br** and to [M] for **InCl_CCTMS**. With regard to Sn(IV) complexes, similar peaks corresponding to [M] and [M − Cl] were detected for both **$SnCl_2$_Br** and **$SnCl_2$_CCTMS**. However, only low abundant [M] peaks were observed. This is in agreement with previous reports. Typically, molecular ions are not detected for Sn(IV) complexes and peaks corresponding to molecular ions diminished by one axial ligand are most abundant in MS spectra for these complexes.[26] Note that [M − 2Cl] was observed in the spectrum of **$SnCl_2$_Br**, yet, it was not detected for **$SnCl_2$_CCTMS**. Peaks around m/z = 817 in the MS spectrum of **$SnCl_2$_CCTMS** could indicate a contamination with hydroxo complexes.

The ^{1}H NMR spectra of **Pd_Br** and **Pt_Br** in $CDCl_3$ were sensitive to concentration. This was attributed to π–π aggregation which is a well known phenomenon for metalloporphyrins.[27] ^{1}H NMR studies on metalloporphyrins reported in the literature demonstrated that the strength of aggregation is dependent on the interaction of the metal ion with the porphyrin π-system. The aggregation was enhanced by the presence of electron-withdrawing substituents on the porphyrin periphery. Thus, in the context of the basic concept of porphyrin aggregation the 5,10-A_2B_2 porphyrins with their intramolecular dipole moments are prone to aggregation effects.

Changes in the β proton signals for **Pd_Br** were observed upon dilution and over time (Fig. 2). More significant changes occurred for β proton signals in the lower field region (>9.4), whereas proton signals in the higher field region (<9.0) were less affected. For analysis we compared three different concentrations. The most concentrated sample (c_0 = 2.6 × 10^{-3} M) exhibited a doublet overlapping with a singlet which after 6 days changed to a broad signal at a similar chemical shift. A ten-fold diluted sample (c_1 = 2.6 × 10^{-4} M) exhibited a singlet and a doublet which appeared in the lower field region in comparison to the signal of the more concentrated sample. The doublet and the singlet shifted slightly into the higher field region over two days. The sample which was further diluted ten-fold (c_2 = 2.6 × 10^{-5} M) also exhibited a singlet and a doublet which were slightly shifted towards the lower field region in comparison to the respective signals of the more concentrated sample (c_1). No changes in the signals of the most diluted sample occurred up to four days. Changes in the lower field β proton signals were also observed for **Pt_Br**. Consistent with the studies on **Pd_Br**, the signals for **Pt_Br** were shifted downfield upon dilution.

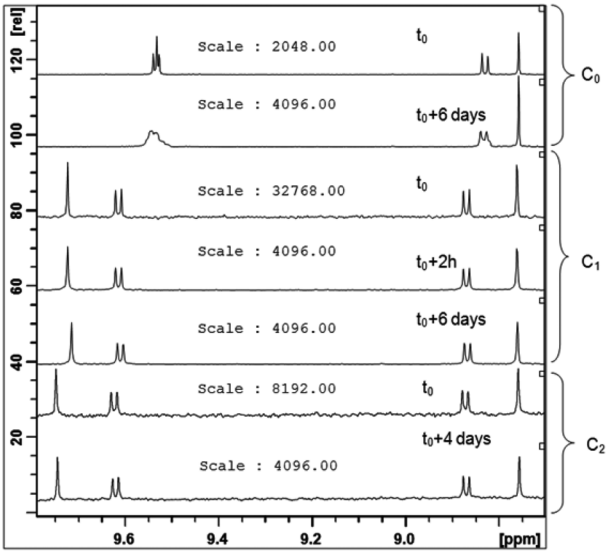

Fig. 2 Low field region of the ^{1}H NMR spectrum showing changes in the β-proton signals of **Pd_Br** upon dilution and over time. c_0 = 2.6 × 10^{-3} M, c_1 = 2.6 × 10^{-4} M and c_2 = 2.6 × 10^{-5} M in $CDCl_3$.

The aggregation properties of **Pd_Br** were studied further with UV-vis spectroscopy. Porphyrins exhibit two characteristic bands in their UV-vis spectra: an intensive Soret band (around 400 nm) and less intense Q-bands (500–650 nm). Aggregation can induce changes to the positions of the absorbances and their intensities.[28] Broadening of absorbances is also indicative of aggregation. The UV-vis spectra of **Pd_Br** were recorded in a 10^{-3}–10^{-6} M concentration range in chloroform, DMF and toluene. No changes in the extinction coefficient ε of the Q-band with concentration were observed in toluene. However, changes were observed in DMF (up to 2.5 × 10^{-4} M) and in chloroform (up to 2.5 × 10^{-5} M) which indicated that aggregation occurred in these solvents.

Linear and nonlinear absorption properties

Ground state absorption features. The ground state absorption spectra of free base and metalated 5,10-A_2B_2 porphyrins for a brominated and TMS-/TIPS-ethynyl substituted series are presented in Fig. 3. The spectra of the TMS-/TIPS-ethynyl series are red-shifted compared to the bromoporphyrins. In both series, the spectra of the metal complexes are bathochromically shifted compared to the free bases. Exceptions include **Pt_Br**, which showed a hypsochromic shift in reference to the free base **H_2_Br** and palladium complexes **Pd_Br** and **Pd_CCTMS** which appear at a similar wavelength to their free

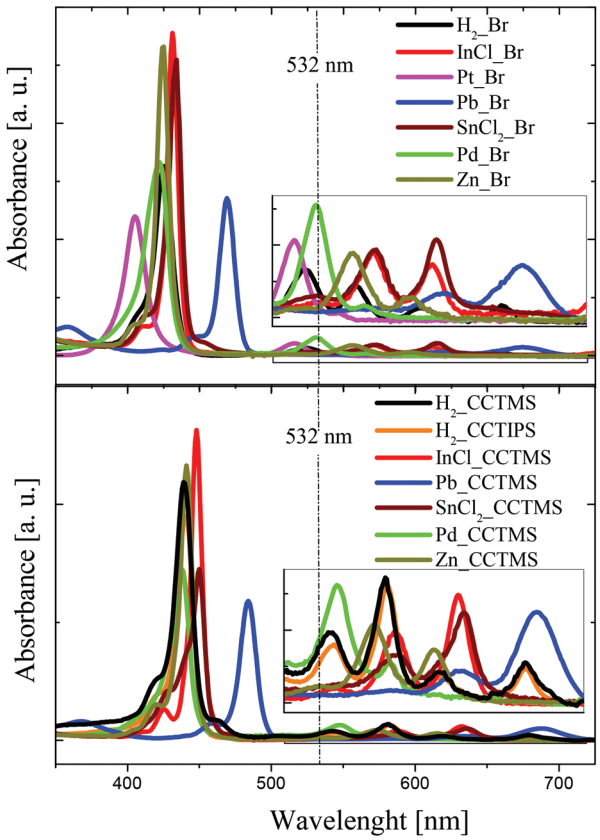

Fig. 3 Ground state absorption spectra of 5,10-A_2B_2 porphyrins in CH_2Cl_2.

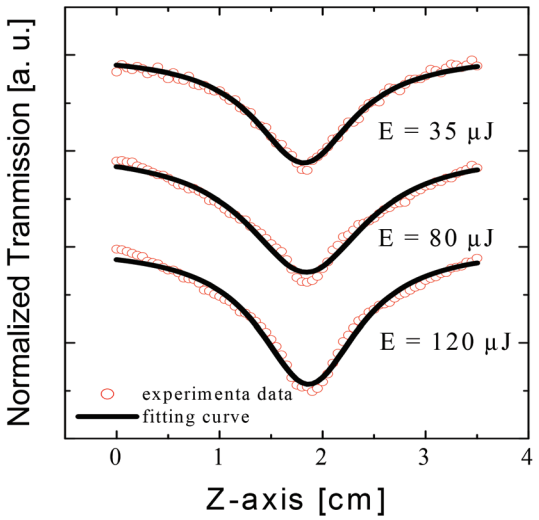

Fig. 4 Illustration of the experimental data obtained for compound **$SnCl_2$_Br** along with fitting curves generated with the analytical expression for the normalized transmission. The theoretical curves provided good fit to low input energy data and diverged for those at higher inputs.

base analogues **H_2_Br** and **H_2_CCTMS**, respectively. The behavior of **Pt_Br** is in agreement with previous reports on platinum porphyrins.[29] The spectra of lead complexes are even more shifted towards longer wavelengths in both series of compounds. As expected, the number of Q-bands is reduced for metalated compounds due to an increase in symmetry. Except for the free base forms, the same metal complexes of both series exhibit similar Q-band characteristics. In both series of compounds, the Soret and Q-band maxima appear at similar wavelengths for the tin and indium complexes. **H_2_CCTMS** and **H_2_CCTIPS** provided very similar UV-vis spectra.

Nonlinear absorption responses and data fitting procedures. A standard means of Z-scan trace analysis, broadly applied in the literature, involves fitting of the experimental data with the analytical expression for the normalized transmission as a function of sample's position along the *Z*-axis to extract effective nonlinear absorption coefficient β_{eff}, which is used for comparative studies.[14,30] It should be mentioned that β_{eff} is not a molecular quantity and thus is expected to depend on concentration and path length (herein, the same experimental conditions were applied for all experiments). The procedure for β_{eff} extraction was used to fit the recorded NLA responses. However, satisfactory fits could only be obtained for low input energy experiments. For the experiments carried out at higher input energies, the fitting curves diverged from the experimental data, to a larger or lesser extent, depending on the compound (see the example in Fig. 4). Thus, the parameter β_{eff} could not be derived for the higher input energy measurements. The values of the effective nonlinear absorption

Table 1 Comparison of linear and nonlinear optical parameters of 5,10-A_2B_2 porphyrins. λ_{max} stands for the Soret band maximum; α_{gr} – linear absorption coefficient at 532 nm; β_{eff} – effective nonlinear absorption coefficient derived for experiments at an input energy of 50 μJ; other parameters as defined in Fig. 5

Compound	λ_{max} [nm]	α_{gr} [cm^{-1}]	β_{eff} [$\times 10^{-8}$ cm W^{-1}]	κ_1	κ_2 [cm^2 GW^{-1}]	I_1 [GW cm^{-2}]	I_2 [GW cm^{-2}]	I_3 [GW^2 cm^{-4}]
H_2_Br	423	3.45	—	0.88	1.7	0.0015	0.90	1.90
InCl_Br	431	1.49	5.7	4.4	6.7	0.17	0.35	1.70
Pd_Br	422	6.32	—	0.75	11.5	0.08	0.07	0.036
Pt_Br	405	2.58	—	10.0	3.8	0.95	0.10	0.28
Pb_Br	470	1.28	6.2	6.5	14.0	0.28	0.90	1.40
$SnCl_2$_Br	434	2.26	6.7	2.8	4.6	0.11	0.68	1.80
Zn_Br	424	1.73	4.8	5.4	5.5	0.30	0.16	2.20
H_2_CCTIPS	440	3.65	8.3	2.5	3.3	0.16	0.30	1.30
H_2_CCTMS	439	3.96	8.1	4.4	2.8	0.45	0.10	2.05
InCl_CCTMS	449	2.06	13.7	5.9	8.5	0.16	0.90	1.90
Pd_CCTMS	438	3.53	18.1	4.2	4.5	0.17	0.30	1.70
Pb_CCTMS	484	1.38	9.4	8.0	12.0	0.21	1.50	1.20
$SnCl_2$_CCTMS	450	1.71	6.4	3.7	8.4	0.13	0.50	0.45
Zn_CCTMS	441	2.3	15.3	5.2	6.5	0.17	0.50	1.70

coefficient β_{eff} derived from low input energy experimental data fitting are given in Table 1.

All open Z-scan data, from experiments carried out at different laser input energies for all compounds, were fitted with the four-level model developed by us recently (Fig. 5).[22] In our previous studies, we examined different models to fit various characters of the NLA responses of 5,10-A_2B_2 porphyrins *e.g.* RSA/SA, SA/RSA/SA or RSA/SA/RSA/SA. We found that, in all cases, the four-level fitted best the recorded response. This brought us to conclusion that, despite different characters of the response, various 5,10-A_2B_2 porphyrins share similar excited state behavior *i.e.* one-photon excited state absorption followed by a simultaneous absorption of two photons from higher excited states. The model assumed fast ISC and high yield for the formation of the triplet states, which should be a valid approximation for macrocycles with heavy atoms in the core or on the molecular periphery.[7,31] Illustration of the model and definition of the parameters used in the fitting are presented in Fig. 5. The model was successfully used to fit the responses of newly synthesized compounds of both series: brominated and the TMS-/TIPS-ethynyl, in toluene (Fig. 6). Best fit parameters used in the modeling of the responses are summarized in Table 1.

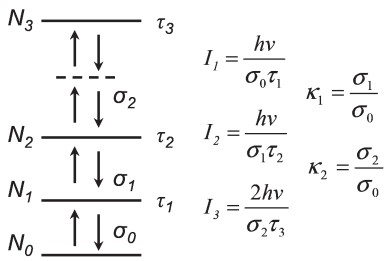

Fig. 5 Illustration of a four-level model used in the fitting NLA response of 5,10-A_2B_2 porphyrins along with the definition of the parameters I_1, I_2, I_3, κ_1 and κ_2. τ_i stands for the lifetime of the i-th state, σ_i for the absorption cross-sections associated with i-th state.[22]

Discussion

The effective nonlinear absorption coefficient β_{eff}, derived from low input energy open Z-scan data, was in the in the range of 4.8–18.1 cm W^{-1} for the compounds studied. The highest values of β_{eff} were obtained for the palladium, indium, zinc and lead complexes from the TMS-ethynyl substituted series. These compounds also exhibited the strongest transmission drop with input intensity, making them most promising for OL applications. The values of β_{eff} obtained were comparable to those reported before for phthalocyanines and porphyrins.[14,30,32]

All of the recorded responses, at a whole range of input energies, were successfully fitted with the four-level model. The model assumes consecutive one- and two-photon excited state absorption (one- + one- + two-photon absorption). This behavior is distinct from that reported for most of the other macrocycles, which is typically explained with third order NLO processes.

A switching from transmission drop to an increase (RSA/SA switch) was observed for **$SnCl_2$_CCTMS** in the higher fluence regime (~6 J cm^{-2}). A similar switch, though at lower input fluence (2 J cm^{-2}), was detected for a platinum complex from the brominated series **Pt_Br** (Fig. 6). An RSA/SA switch at comparable low input fluence was also observed for **Pd_Br** which exhibited an overall SA/RSA/SA character of the response. Typically, an RSA/SA switch does not occur in the ns regime for macrocyclic dyes but has been reported to arise for different materials under ps pulses.[33] In these cases the RSA/SA switch in the ps regime was attributed to a contribution of poorly absorbing higher excited states to the measured NLA signal.

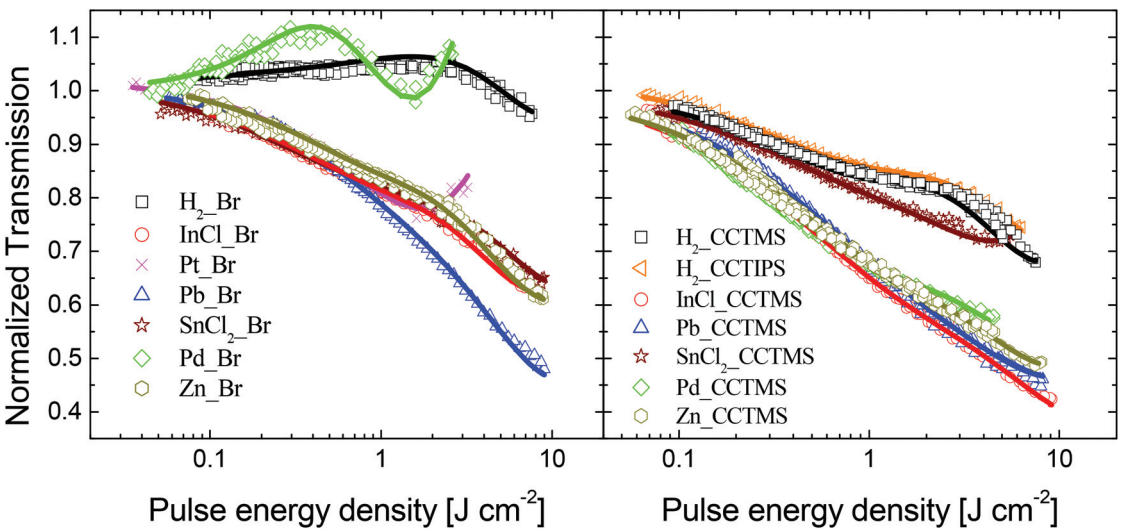

Fig. 6 Comparison of the nonlinear responses along with fitting curves generated based on the four-level model for brominated (left panel) and TMS-/TIPS-ethynyl (right panel) substituted 5,10-A_2B_2 porphyrins.

With regard to the four-level model, the RSA/SA switch can be explained in a similar way. As demonstrated before,[22] absorption arising from state N_3 is negligible, and thus contribution of the absorptive process from these states can lead to RSA/SA. It should be noted that the four-model model applied neglects absorption arising from N_3 but does not neglect the population of N_3. The fitting parameter I_3, which is a saturation intensity of TPA, was lower for **Pt_Br**, **Pd_Br** and **$SnCl_2$_CCTMS** compared to other porphyrins. The lifetime of state $N_3 - \tau_3 \sim 1/(\sigma_0\kappa_2 I_3)$. Since $\sigma_0 = \alpha_{gr}/N$ and concentration N was the same for all compounds studied $\tau_3 \sim 1/(\alpha_{gr}\kappa_2 I_3)$. The ratios of the lifetimes of state $N_3 - \tau_3$ for compounds **Pt_Br**, **Pd_Br** and **$SnCl_2$_CCTMS** to the lifetimes τ_3 of other porphyrins were evaluated. Values in the range of 4.1–12.1 and 4.3–12.7 were obtained for **Pt_Br** and **Pd_Br** respectively; for **$SnCl_2$_CCTMS**, with a switch occurring in the higher fluence regime, lower ratios of 1.7–5.1 were found. Longer lifetimes of higher excited states will lead to higher population of these states and this triggers further undesirable poorly absorptive processes, resulting in SA behavior for compounds **Pt_Br**, **Pd_Br** and **$SnCl_2$_CCTMS**.

Compound **H_2_Br** exhibited weak SA for fluences up to 2 J cm^{-2} to then switch to RSA in the higher fluence range. A SA/RSA switch was observed also for **Pd_Br** but at much lower fluence of 0.4 J cm^{-2}. Typically, SA is observed at excitation wavelengths close to/at ground state absorption peaks. The experimental wavelength of 532 nm was situated in the Q-band peak regime for **H_2_Br** and equal to the Q-band maximum for **Pd_Br**. SA/RSA has been reported before for other macrocycles in the ns regime and was attributed to the contribution of more absorptive higher excited states at higher fluences.[34] The switch observed for **H_2_Br** and **Pd_Br** can be explained in a similar way. The ratios of the absorption cross-sections of the following excited states (N_1 and N_2) to ground state absorption cross-section took values $\kappa_1 < 1$ and $\kappa_2 > 1$ for both compounds. However, according to the four-level model which provided a good fit to experimental data for **H_2_Br** and **Pd_Br**, in contrast to previous reports, RSA is due to TPA arising from higher excited states rather than to one photon ESA.

In all series of compounds, the free bases **H_2_Br** and **H_2_CCTMS** (and **H_2_CCTIPS**, too) exhibited the weakest transmission drop in comparison to the metal complexes (an exception is **Pd_Br** in which transmission drop was comparable to that exhibited by **H_2_Br**). This observation agrees with previous reports.[5,15] Insertion of metals into the central core is usually an efficient way to improve the OL performance of macrocyclic dyes due to a heavy atom effect through the enhancement of the ISC rate and the quantum yield for the triplet states. Both **H_2_CCTIPS** and **H_2_CCTMS** showed very similar NLA responses. Thus, introduction of different alkyl groups onto the silicon atom had no effect on the NLA response.

The effect of the metal on the OL efficiency was different for the two series of porphyrins. This finding is in agreement with other reports.[5] It indicates that both structural features, *i.e.* the metal and the substituents, must be tailored simultaneously to maximize the OL performance. Here, **InCl_Br**, **$SnCl_2$_Br** and **Zn_Br** exhibited very similar NLA responses. The lead compound **Pb_Br** provided the best OL efficiency amongst the bromoporphyrins. In the TMS-ethynyl series the tin complex exhibited weaker OL efficiency than the palladium compound, which in turn was outperformed by the zinc, lead and indium complexes. The latter three compounds provided very similar OL curves. In conclusion, the lead complexes were consistently strong positive nonlinear absorbers within a series.[7,15] Indium and zinc complexes provided very similar OL curves within each series. Thus, the metal effect is less important than that exerted by substituents for these compounds.

With the exception of tin, all other complexes from the TMS-ethynyl substituted series outperformed their metal analogues from the brominated series. Even though the lead brominated compound **Pb_Br** exhibited a comparable minimal transmission to that recorded for the strongest nonlinear absorbers from the TMS-ethynyl series (**Pb_CCMTS**, **Zn_CCTMS** and **InCl_CCTMS**), its OL performance was suppressed in reference to those compounds over a lower fluence range (Fig. 6). This indicates that replacement of the heavy bromine atoms at two *meso* positions in 5,10-A_2B_2 porphyrins with conjugated groups enhances the OL efficiency. TMS- and TIPS-ethynyl tetrasubstituted porphyrins were previously reported as very promising materials for OL application[7,15] and our studies confirm the potential of the TMS-ethynyl *meso* substituent for generating an efficient OL effect. Only a few studies dealt with the effect of bromination on NLA.[13,35] Introduction of bromine atoms at both the *meso* and β positions was reported to enhance the ISC rate and the quantum yield for triplet states up to unity.[31] (2,3,7,8,12,13,17,18-Octabromo-5,10,15,20-tetraphenylporphyrinato)zinc(II) was shown to have especially strong positive NLA with an OL efficiency comparable to the advanced phthalocyanine chloro{tetra(*tert*-butyl)-phthalocyaninato}indium(III).[35] Compared to TMS-ethynyl substituted 5,10-A_2B_2 compounds the brominated porphyrins exhibited weaker OL efficiency and thus have less potential for green light OL.

Next we compared the fitting parameters obtained for different 5,10-A_2B_2 porphyrins. Normalized transmission at a fluence of 5 J cm^{-2} was plotted together with κ_1 and κ_2 for different compounds (Fig. 7). Data for compounds **Pd_Br** and **Pt_Br** are not presented in the plots. Measurement at higher input energies (covering a higher fluence range) did not provide any reproducible data for these compounds. Evidently, normalized transmission correlates to both parameters – κ_1 and κ_2. Additionally, κ_1 follows a trend similar to κ_2. The one- and two-photon excited state absorption cross-sections σ_1 and σ_2, respectively, were then recalculated from $\sigma_i = \kappa_i\sigma_0$ where $\sigma_0 = \alpha_{gr}/N$, and plotted for the compounds studied. Since the concentration N was the same for all the compounds $\sigma_1 \sim \kappa_1\alpha_{gr}$ and $\sigma_2 \sim \kappa_2\alpha_{gr}$. The normalized transmission correlates to both σ_1 and σ_2. However, it is likely that the correlation with the latter parameters is stronger. TMS-ethynyl substituted metalated complexes exhibited higher σ_2 than brominated compounds. An exception was the lead complex **Pb_Br**. Except for the tin complex, TMS-ethynyl substituted porphyrins also

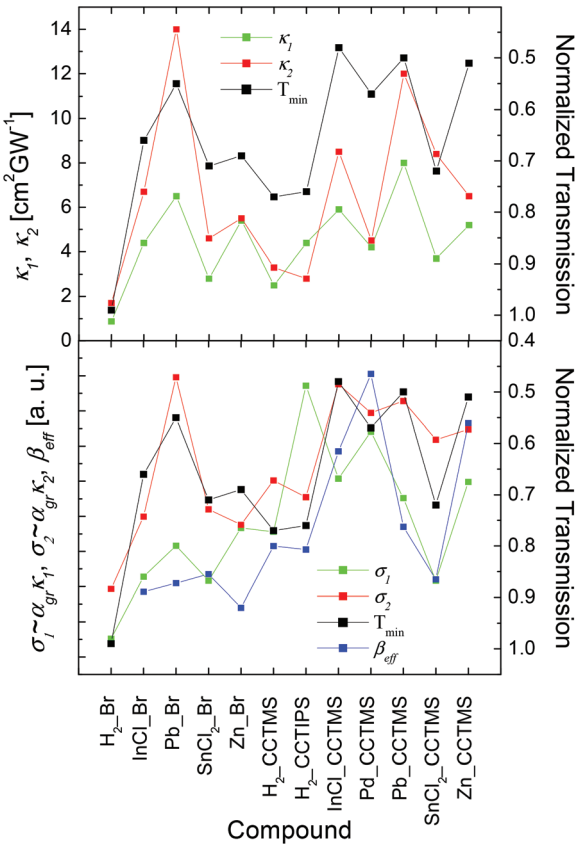

Fig. 7 Parameters κ_1 and κ_2 plotted along with normalized transmission at input fluence of 5 J cm^{-2} (top panel) and a similar plot for σ_1 and σ_2 and β_{eff} (lower panel).

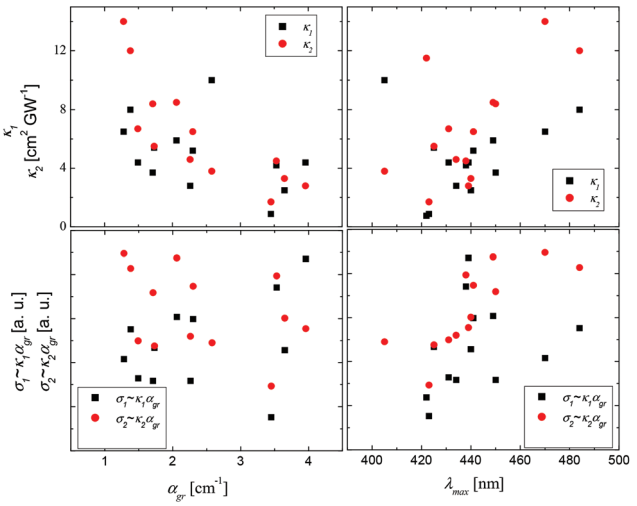

Fig. 8 Parameters κ_1 and κ_2 plotted *versus* the linear absorption coefficient α_{gr} (upper left) and the Soret band maximum (upper right). $\sigma_1 \sim \kappa_1\alpha_{gr}$ and $\sigma_2 \sim \kappa_2\alpha_{gr}$ *versus* α_{gr} (lower left) and *versus* λ_{max} (lower right). Data for **Pd_Br** are not shown.

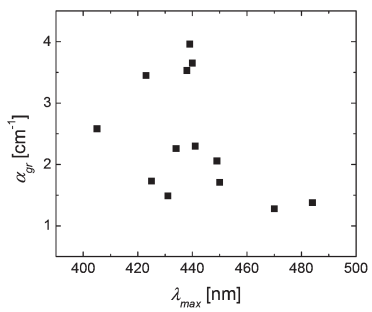

Fig. 9 Linear absorption coefficient α_{gr} *versus* Soret band maximum λ_{max} for 5,10-A$_2$B$_2$ porphyrins. Data for compound **Pd_Br** are not shown.

exhibited higher σ_1 than the other compounds. Overall, there seems to be a correlation between σ_1 and σ_2 suggesting that compounds which exhibit a higher excited state absorption cross-section of one-photon process σ_1 tend to exhibit a higher excited state absorption cross-section of the consecutive two-photon process σ_2, too.

It can be seen from Fig. 7 (lower panel) that β_{eff} correlates to the one-photon excited state absorption cross-section σ_1. β_{eff} was derived from low input energy experiments. Under such experimental conditions, the NLA response of 5,10-A$_2$B$_2$ porphyrins should be dominated by one-photon ESA. Therefore one can expect these parameters to be correlated.

Parameters κ_1, κ_2 and $\sigma_1 \sim \kappa_1\alpha_{gr}$ and $\sigma_2 \sim \kappa_2\alpha_{gr}$ were plotted against the linear absorption coefficient α_{gr} and the Soret band maximum λ_{max} (Fig. 8). Both parameters κ_1 and κ_2 increase with λ_{max} and decrease with α_{gr}. The opposite trend observed for κ_1 and κ_2 with respect to λ_{max} and α_{gr} can be associated with a rough correlation between the latter two parameters (Fig. 9). α_{gr} generally appears to decrease with λ_{max}. This could be understood since roughly speaking the red shift of the linear absorption spectra (*i.e.* an increase in λ_{max}) causes the experimental wavelength of 532 nm to move further apart from the Q-band region of high linear absorption. No specific trend could be observed for $\sigma_1 \sim \kappa_1\alpha_{gr}$ and $\sigma_2 \sim \kappa_2\alpha_{gr}$ plotted against α_{gr}. However, part of the data plotted *versus* λ_{max} tended to increase with increasing λ_{max}. This is in agreement with data in the literature. Broadband studies carried out by McEwan *et al.* showed the excited state absorption cross-section to reach its maximum close to the Soret band and to decrease upon moving closer to the Q-band region for porphyrins.[7] For TMS-ethynyl substituted compounds, in which the UV-vis spectra are more shifted towards longer wavelengths, the excitation wavelength of 532 nm is situated closer to the Soret band. These compounds exhibit higher values of the excited state absorption cross-section than porphyrins from the brominated series, for which 532 nm is closer to the Q-band area. McEwan *et al.* also proposed that there is a correlation between the position of the Soret band maximum *versus* the experimental wavelength and the OL efficiency, *i.e.* the closer the Soret band is to 532 nm the stronger is the transmission drop. We noted a similar trend for structurally diverse porphyrins of the 5,15-A$_2$B$_2$, 5,15-A$_2$BC series before.[14,36] The same observation can be applied to the 5,10-A$_2$B$_2$ compounds studied, *i.e.*, both κ_1 and κ_2 increase with the maximum of the Soret band.

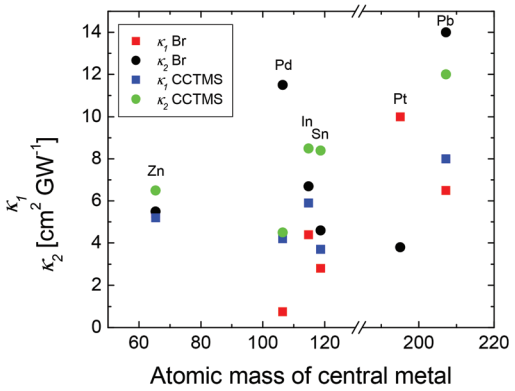

Fig. 10 The ratio of the excited to ground states absorption cross-section κ_1 and κ_2 *versus* atomic mass of the central metal.

Finally, κ_1 and κ_2 were plotted against the atomic mass of the central metal for the brominated and TMS-ethynyl substituted compounds (Fig. 10). Previously, O'Flaherty *et al.* reported that although no definite correlation could be observed between the ratio of the excited to ground state absorption cross-sections κ and the atomic mass of the central atom for metalated phthalocyanines, the parameter κ generally appeared to increase with the atomic mass of the metal.[30] A similar trend can be observed for the 5,10-A_2B_2 porphyrins with regard to parameters κ_1 and κ_2. However, the correlation tends to be stronger if one analyzes the variation of parameter κ_1 or κ_2 for a given series of compounds, *i.e.* brominated or TMS-ethynyl substituted compounds with the exception: parameter κ_2 from the brominated series.

Experimental

Synthesis

Instrumentation and standard techniques for materials characterization were as described before.[37] Compounds **Zn_Br**, **Pd_Br**, **H_2_CCTMS** and **Zn_CCTMS** were obtained as reported before.[22]

General procedure A – Sonogashira coupling. A Schlenk-tube was filled with Ar and charged with brominated porphyrin (1 equiv.), in dry THF–NEt_3 (1 : 3, v : v). The solution was degassed by three freeze–pump–thaw cycles and placed under Ar again. Trimethysilylacetylene (TMS-acetylene) or triisopropylsilylacetylene (TIPS-acetylene) (5 equiv.), copper(I) iodine (0.25 equiv.) and $Pd(PPh_3)_2Cl_2$ (0.1 or 0.25 equiv.) were added, and the reaction mixture was stirred at room temperature until the starting material was consumed. Then CH_2Cl_2 (30 mL) was added and the solution was washed with water and dried over $MgSO_4$. Further purification utilized column chromatography.

Chloro{5,10-dibromo-15,20-di(*p*-tolyl)porphyrinato}indium(III) (InCl_Br). 5,10-Dibromo-15,20-di(*p*-tolyl)porphyrin (**H_2_Br**) (100 mg, 0.154 mmol), $InCl_3$ (332 mg, 1.501 mmol) and sodium acetate (1.312 g, 0.015 mol) were dissolved in glacial acetic acid (50 mL). The reaction mixture was heated at reflux for 24 h. The solvent was removed under reduced pressure and the solid residue was dissolved in DCM. The solution was extracted with an aqueous solution of $NaHCO_3$ (5% w/v). The organic phase was washed twice with a saturated aqueous solution of NaCl and dried over $MgSO_4$. The solvent was removed and the solid residue was purified. Chromatographic separation was performed on silica gel. Traces of free base porphyrins were eluted with CH_2Cl_2–*n*-hexane (1 : 2, v : v) followed by elution of the metalloporphyrin with CH_2Cl_2 to yield 119 mg (0.150 mmol, 98%) of a dark blue solid. M.p. > 300 °C; R_f = 0.2 (SiO_2, $CHCl_3$); ^{1}H NMR (400 MHz, $CDCl_3$): δ = 2.75 (s, 6H, CH_3), 7.59 (d, 2H, J = 7.6 Hz, H_{arom}), 7.65 (d, 2H, J = 7.6 Hz, H_{arom}), 7.97 (d, 2H, J = 7.6 Hz, H_{arom}), 8.23 (d, 2H, J = 7.6 Hz, H_{arom}); 9.04 (s, 2H, H_β), 9.14 (d, 2H, J = 4.8 Hz, H_β), 9.85 (d, 2H, J = 4.7 Hz, H_β), 9.93 ppm (s, 2H, H_β); ^{13}C NMR (150.90 MHz, $CDCl_3$): δ = 21.5, 105.0, 123.5, 127.6, 127.7, 133.5, 133.9, 134.1, 134.5, 134.7, 135.0, 138.1, 138.2, 149.2, 149.3 ppm; UV-vis (CH_2Cl_2): λ_{max} (log ε) = 431 (3.86), 571 (2.69), 612 nm (2.64); HRMS (MALDI LD$^+$): calcd for $C_{34}H_{22}N_4ClBr_2In$ $[M]^+$ 793.8938, found 793.8903.

{5,10-Dibromo-15,20-di(*p*-tolyl)porphyrinato}platinum(II) (Pt_Br). Porphyrin **H_2_Br** (30 mg, 0.046 mmol) and $PtCl_2$ (36 mg, 0.135 mmol) were heated in benzonitrile (10 mL) under Ar at 170 °C. The progress of the reaction was monitored by TLC using $CHCl_3$–*n*-hexane (1 : 4). Upon completion after 12 h the solution was cooled to room temperature and MeOH was added to precipitate the product, which was filtered off and isolated after passage through a plug of silica gel using $CHCl_3$ as an eluent. The solvent was removed under reduced pressure and the product was recrystallized from $CHCl_3$/MeOH to yield 23 mg (0.0277 mmol, 60%) of bright red crystals. M.p. = 292–293 °C; R_f = 0.25 (SiO_2, $CHCl_3$–*n*-hexane 1 : 4, v/v); ^{1}H NMR (400 MHz, $CDCl_3$): δ = 2.73 (s, 6H, CH_3), 7.58 (d, 4H, J = 7.6 Hz, H_{arom}), 8.00 (d, 4H, J = 7.6 Hz, H_{arom}), 8.69 (s, 2H, H_β), 8.74 (d, 2H, J = 5.3 Hz, H_β), 9.25 (s, 2H, H_β), 9.36 ppm (d, 2H, J = 5.3 Hz, H_β); ^{13}C NMR (100.6 MHz, $CDCl_3$): δ = 21.6, 114.8, 123.0, 127.7, 128.6, 128.7, 131.2, 131.6, 133.8, 137.8, 137.9, 139.0, 139.3, 141.4, 141.5 ppm; UV-vis (CH_2Cl_2): λ_{max} (log ε) = 405 (5.38), 516 nm (4.33); HRMS (MALDI LD$^+$): calcd for $C_{34}H_{22}N_4Br_2Pt$ $[M]^+$ 838.9857, found 838.9861.

{5,10-Dibromo-15,20-di(*p*-tolyl)porphyrinato}lead(II) (Pb_Br). A solution of 90 mg (0.139 mmol) of **H_2_Br** and 1.125 g (2.776 mmol) of $Pb(acac)_2$ in 40 mL of toluene–MeOH (1 : 1, v : v) was stirred at room temperature for 30 min. The reaction was monitored by UV-vis spectroscopy. As soon as the reaction was completed water was added and the mixture was extracted with dichloromethane. The organic phase was subsequently washed twice with H_2O and dried over $MgSO_4$. The solvent was removed under reduced pressure and the product was recrystallized from CH_2Cl_2/MeOH to yield 118 mg (0.138 mmol, 99%) of a dark green product. M.p. > 300 °C; R_f = 0.25 (Al_2O_3, $CHCl_3$–*n*-hexane 3 : 20, v/v); ^{1}H NMR (400 MHz, $CDCl_3$): δ = 2.74 (s, 6H, CH_3), 7.58 (s, 4H, H_{arom}), 8.06 (br, 4H, H_{arom}), 8.91 (s, 2H, H_β), 8.99 (d, 2H, J = 4.7 Hz, H_β), 9.74 (d, 2H, J = 4.7 Hz, H_β), 9.85 ppm (s, 2H, H_β); ^{13}C NMR (100.6 MHz, $CDCl_3$): δ = 21.6, 105.3, 124.0, 127.4, 127.6, 132.8, 132.9, 133.7, 133.8,

134.4, 137.5, 139.3, 149.0, 149.1, 150.1 ppm; UV-vis (CH_2Cl_2): λ_{max} (log ε) = 358 (4.62), 470 (5.43), 623 (3.76), 669 nm (4.15); HRMS (MALDI LD$^+$): calcd for $C_{34}H_{22}N_4Br_2Pb$ $[M]^+$ 851.9978, found 851.9951.

Dichloro{5,10-dibromo-15,20-di(*p*-tolyl)porphyrinato}tin(IV) (SnCl$_2$_Br). Porphyrin **H$_2$_Br** (180 mg, 0.278 mmol) and $SnCl_2$ (526 mg, 2.774 mmol) were dissolved in 15 mL DMF and heated to reflux for 1.5 h. The solvent was removed under reduced pressure and the product was isolated after passage through a plug of alumina using $CHCl_3$ as an eluent. The solution was concentrated and the product was precipitated out *via* addition of MeOH. After filtration the product was washed with MeOH and dried to yield 193 mg (0.231 mmol, 83%) of a dark blue product. M.p. > 300 °C; R_f = 0.8 (Al_2O_3, $CHCl_3$); ^{1}H NMR (400 MHz, $CDCl_3$): δ = 2.77 (s, 6H, C*H*$_3$), 7.66 (d, 4H, J = 7.6 Hz, H_{arom}), 8.17 (d, 4H, J = 7.6 Hz, H_{arom}), 9.17 (s, 2H, H_β), 9.28 (d, 2H, J = 4.7 Hz, H_β), 9.98 (d, 2H, J = 4.7 Hz, H_β), 10.10 ppm (s, 2H, H_β); ^{13}C NMR (100.6 MHz, $CDCl_3$): δ = 21.6, 104.3, 123.1, 128.0, 133.5, 134.0, 134.4, 134.9, 137.0, 138.9, 146.1, 146.2, 147.3 ppm; UV-vis (CH_2Cl_2): λ_{max} (log ε) = 434 (5.69), 570 (4.27), 615 nm (4.31); HRMS (MALDI LD$^+$): calcd for $C_{34}H_{22}N_4ClBr_2Sn$ $[M - Cl]^+$ 798.8922, found 798.894.

5,10-Bis[(triisopropylsilyl)ethynyl]-15,20-di(*p*-tolyl)porphyrin (H$_2$_CCTIPS). Following the general procedure A, 30 mg (0.046 mmol) of porphyrin **H$_2$_Br**, 0.05 mL (0.230 mmol) of TIPS-acetylene, 2 mg (0.012 mmol) of CuI and 8 mg (0.011 mmol) of $Pd(PPh_3)_2Cl_2$ in 12 mL of THF–NEt_3 (1 : 3, v : v) after 12 h gave 19 mg (0.022 mmol, 48%) of a dark green solid after purification by column chromatography on silica gel (CH_2Cl_2–*n*-hexane 1 : 2 v : v). M.p. > 300 °C; R_f = 0.45 (SiO_2, CH_2Cl_2–*n*-hexane 1 : 3, v/v); ^{1}H NMR (400 MHz, $CDCl_3$): δ = −2.08 (br, 2H, N*H*), 1.41–1.56 (m, 42H, TIPS-*H*), 2.72 (s, 6H, C*H*$_3$), 7.57 (d, 4H, J = 7.6 Hz, H_{arom}), 8.05 (d, 4H, J = 7.6 Hz, H_{arom}), 8.74 (s, 2H, H_β), 8.87 (d, 2H, J = 4.7 Hz, H_β), 9.63 (d, 2H, J = 4.7 Hz, H_β), 9.63 ppm (s, 2H, H_β); ^{13}C NMR (150.90 MHz, $CDCl_3$): δ = 11.9, 19.1, 21.5, 98.9, 100.2, 108.4, 122.8, 127.5, 134.2, 137.6, 138.6 ppm; UV-vis (CH_2Cl_2): λ_{max} (log ε) = 440 (5.67), 545 (4.20), 583 (4.51), 619 (3.84), 679 nm (3.97); HRMS (MALDI LD$^+$): calcd for $C_{56}H_{67}N_4Si_2$ $[M + H]^+$ 851.4904, found 851.4901.

Chloro{5,10-di(*p*-tolyl)-15,20-di[(trimethylsilyl)ethynyl]-porphyrinato}indium(III) (InCl_CCTMS). Following the general procedure A, 100 mg (0.126 mmol) of porphyrin **InCl_Br**, 0.087 mL (0.627 mmol) of TMS-acetylene, 6 mg (0.031 mmol) of CuI and 22 mg (0.031 mmol) of $Pd(PPh_3)_2Cl_2$ in 40 mL of THF–NEt_3 (1 : 3, v : v) after 24 h gave 16.7 mg (0.020 mmol, 16%) of a purple solid after purification by column chromatography on silica gel (THF–*n*-hexane 3 : 17 v : v). M.p. > 300 °C; R_f = 0.2 (SiO_2, THF–*n*-hexane 1 : 4, v/v); ^{1}H NMR (400 MHz, $CDCl_3$): δ = 0.67 (s, 18H, C*H*$_3$), 2.75 (s, 6H, C*H*$_3$), 7.58 (d, 2H, J = 7.6 Hz, H_{arom}), 7.65 (d, 2H, J = 7.6 Hz, H_{arom}), 7.95 (d, 2H, J = 7.6 Hz, H_{arom}), 8.25 (d, 2H, J = 7.6 Hz, H_{arom}), 8.97 (s, 2H, H_β), 9.09 (d, 2H, J = 4.7 Hz, H_β), 9.79 (d, 2H, J = 4.7 Hz, H_β), 9.90 ppm (s, 2H, H_β); ^{13}C NMR (150.90 MHz, $CDCl_3$): δ = 0.3, 21.5, 101.5, 103.5, 106.1, 124.5, 127.6, 127.7, 131.6, 132.6, 133.0, 134.0, 134.1, 135.0, 138.0, 138.2, 149.0, 149.8, 151.5, 152.0 ppm; UV-vis (CH_2Cl_2): λ_{max} (log ε) = 449 (5.82), 588 (4.29), 632 nm (4.47); HRMS (MALDI LD$^+$): calcd for $C_{44}H_{40}N_4ClInSi_2$ $[M]^+$ 830.1522, found 830.1519.

{5,10-Di(*p*-tolyl)-15,20-[(trimethylsilyl)ethynyl]-porphyrinato}-palladium(II) (Pd_CCTMS). Following the general procedure A, 50 mg (0.066 mmol) of porphyrin **Pd_Br**, 0.046 ml (0.326 mmol) of trimethylsilylacetylene, 3 mg (0.016 mmol) of CuI and 4.6 mg (0.006 mmol) of $Pd(PPh_3)_2Cl_2$ in 20 mL of THF–NEt_3 (1 : 3, v : v) after 12 h gave 30.2 mg (0.038 mmol, 57%) of a red solid after purification by column chromatography on silica gel (EtOAc–*n*-hexane = 1 : 24, v : v). M.p. > 300 °C; R_f = 0.56 (SiO_2, EtOAc–*n*-hexane 1 : 19, v/v); ^{1}H NMR (400 MHz, $CDCl_3$): δ = 0.63 (s, 18H, C*H*$_3$), 2.72 (s, 6H, C*H*$_3$), 7.56 (d, 4H, J = 7.8 Hz, H_{arom}), 8.01 (d, 4H, J = 7.8 Hz, H_{arom}), 8.72 (s, 2H, H_β), 8.83 (d, 2H, J = 4.9 Hz, H_β), 9.56 (d, 2H, J = 4.9 Hz, H_β), 9.67 ppm (s, 2H, H_β); ^{13}C NMR (150.90 MHz, $CDCl_3$): δ = 0.1, 21.4, 101.6, 101.9, 105.7, 123.8, 127.4, 129.9, 130.8, 130.9, 131.9, 133.8, 137.5, 138.1, 141.2, 141.8, 143.5, 143.8 ppm; UV-vis (CH_2Cl_2): λ_{max} (log ε) = 438 (2.68), 547 (1.81), 584 (1.59); HRMS (ES$^+$): calcd for $C_{44}H_{41}N_4PdSi_2$ $[M + H]^+$ 787.1905, found 787.1921.

{5,10-Di(*p*-tolyl)-15,20-di[(trimethylsilyl)ethynyl]-porphyrinato}-lead(II) (Pb_CCTMS). Following the procedure given for **Pb_Br**, 73 mg (0.106 mmol) of porphyrin **H$_2$_CCTMS** and 433 mg (1.069 mmol) of $Pb(acac)_2$ in 30 mL of toluene–MeOH (1 : 1, v : v) were stirred for 40 min at room temperature. Recrystallization yielded 89 mg (0.100 mmol, 94%) of a dark green product. M.p. > 300 °C; R_f = 0.2 (Al_2O_3, $CHCl_3$–*n*-hexane 3 : 20, v/v); ^{1}H NMR (400 MHz, $CDCl_3$): δ = 0.65 (s, 18H, C*H*$_3$), 2.73 (s, 6H, C*H*$_3$), 7.58 (br, 4H, H_{arom}), 7.91 (br, 2H, H_{arom}), 8.19 (br, 2H, H_{arom}), 8.86 (s, 2H, H_β), 8.96 (d, 2H, J = 4.7 Hz, H_β), 9.69 (d, 2H, J = 4.7 Hz, H_β), 9.81 ppm (s, 2H, H_β); ^{13}C NMR (150.90 MHz, $CDCl_3$): δ = 0.2, 21.4, 101.0, 101.2, 107.5, 125.4, 127.2, 127.4, 130.4, 131.6, 132.2, 133.3, 134.2, 137.3, 139.2, 148.5, 149.5, 151.4, 152.0 ppm; UV-vis (CH_2Cl_2): λ_{max} (log ε) = 368 (4.61), 484 (5.47), 636 (3.94), 687 nm (4.40); HRMS (MALDI LD$^+$): calcd for $C_{44}H_{40}N_4Si_2Pb$ $[M]^+$ 888.2558, found 888.2598.

Dichloro{5,10-(*p*-tolyl)-15,20-di[(trimethylsilyl)ethynyl]-porphyrinato}tin(IV) (SnCl$_2$_CCTMS). Porphyrin **H$_2$_CCTMS** (67 mg, 0.098 mmol) and $SnCl_2$ (186 mg, 0.981 mmol) in 7 mL of DMF were heated at reflux for 1.5 h. The solvent was removed under reduced pressure and the solid residue was dissolved in CH_2Cl_2. The solution was washed twice with water and with a saturated, aqueous solution of NaCl and dried over $MgSO_4$ to yield 70 mg (0.0804 mmol, 89%) of a blue solid. M.p. > 300 °C; ^{1}H NMR (400 MHz, $CDCl_3$): δ = 0.67 (s, 18H, C*H*$_3$), 2.76 (s, 6H, C*H*$_3$), 7.64 (d, 4H, J = 8.2 Hz, H_{arom}), 8.17 (d, 4H, J = 8.2 Hz, H_{arom}), 9.09 (s, 2H, H_β), 9.22 (d, 2H, J = 4.7 Hz, H_β), 9.89 (d, 2H, J = 4.7 Hz, H_β), 10.01 ppm (s, 2H, H_β); ^{13}C NMR (150.90 MHz, $CDCl_3$): δ = 0.3, 21.5, 101.5, 103.5, 106.1, 124.5, 127.6, 127.7, 131.6, 132.6, 133.0, 134.0, 134.1, 135.0, 138.0, 138.2, 149.0, 149.8, 151.5, 152.0 ppm; UV-vis (CH_2Cl_2): λ_{max} (log ε) = 450 (5.31), 591 (3.87), 636 nm (4.15); HRMS (MALDI LD$^+$): calcd for $C_{44}H_{40}N_4Si_2ClSn$ $[M - Cl]^+$ 835.1502, found 835.1536.

NLO measurements

The open Z-scan technique[38] was used to measure NLA of the 5,10-A_2B_2 porphyrins in toluene (2.5×10^{-4} M, path length: 1 mm) as described before.[22] Each sample was investigated at different laser input energies (from ~35 μJ until reproducible data could be obtained ~200 μJ with an average step of about 20 μJ).

Conclusions

Two series of 5,10-A_2B_2 porphyrins both bearing *p*-tolyl as substituent A and bromine or TMS-ethynyl groups as substituent B with different metals in the central core were investigated for their NLA properties with an open Z-scan technique. The NLA responses were successfully fitted with a four-level model where one photon ESA is followed by instantaneous two-photon absorption processes. Most of the compounds exhibited a transmission drop with input fluence. An undesirable for OL applications, a RSA/SA switch, was found for the platinum complex of a bromoporphyrin at very low input fluence and at higher input for a tin complex of TMS-ethynyl substituted porphyrins. This was associated with longer lifetimes of the higher excited states triggering further weakly absorptive processes. A similar switch was also observed at low fluence for palladium bromoporphyrin which exhibited an overall SA/RSA/SA character of the response. The RSA/SA switch could be explained in the same manner as above. Besides palladium bromoporphyrin, an SA/RSA switch was detected for a free base bromoporphyrin. Both compounds exhibited high linear absorption at experimental wavelength.

The TMS-ethynyl *meso* substituent was found to be a more promising OL group than a bromine atom at equivalent positions. Consistently, the lead complexes were found to be strong positive nonlinear absorbers in both series of compounds. Only smaller differences were found for the NLA responses of tin, indium and zinc brominated complexes and for the indium, zinc and lead porphyrins of the TMS-ethynyl substituted series. Thus, the substituent effect is stronger than the central metal effect. Excited state absorption cross-sections were found to increase with longer wavelength positions of the Soret band maxima. The ratio of the excited to ground state absorption cross-sections was found to increase with the atomic mass of the central metal. The studies showed that modification of the porphyrin periphery has a significant impact on its excited state structure. The 5,10-A_2B_2 regiochemical substitution pattern provides compounds with interesting NLA behavior distinct from that of *meso* tetrasubstituted porphyrins or 5,15-A_2B_2 or 5,15-A_2BC-type systems. The central metal significantly improves the NLA of 5,10-A_2B_2 porphyrins. Both the central metal and the *meso* substituents must be tailored simultaneously to maximize the OL performance.

Acknowledgements

This work was supported by a grant from Science Foundation Ireland (SFI P.I. 09/IN.1/B2650). J.W. acknowledges the financial support from the 100-Talent Program of Chinese Academy of Sciences, the National Natural Science Foundation of China (NSFC, No. 61178007), and Science and Technology Commission of Shanghai Municipality (STCSM Nano Project, No. 11nm0502400, Pujiang Talent Program 12PJ1409400). The authors would like to thank Dr Eimear Finnigan for his help with the manuscript.

Notes and references

1 T. Popmintchev, M. C. Chen, P. Arpin, M. M. Murnane and H. C. Kapteyn, The attosecond nonlinear optics of bright coherent X-ray generation, *Nat. Photonics*, 2010, **4**, 822–832.
2 K. Itoh, W. Watanabe and Y. Ozeki, Nonlinear ultrafast focal-point optics for microscopic imaging, manipulation, and machining, *Proc. IEEE*, 2009, **97**, 1011–1030.
3 M. O. Senge, M. Fazekas, E. G. A. Notaras, W. J. Blau, M. Zawadzka, O. B. Locos and E. M. N. Mhuircheartaigh, Nonlinear optical properties of porphyrins, *Adv. Mater.*, 2007, **19**, 2737–2774.
4 G. de la Torre, P. Vaquez, F. Agullo-Lopez and T. Torres, Role of structural factors in the nonlinear optical properties of phthalocyanines and related compounds, *Chem. Rev.*, 2004, **104**, 3723–3750.
5 M. Calvete, G. Y. Yang and M. Hanack, Porphyrins and phthalocyanines as materials for optical limiting, *Synth. Met.*, 2004, **141**, 231–243.
6 D. Dini, G. Y. Yang and M. Hanack, Porphyrins, phthalocyanines and related compounds as materials for optical limiting, *Targets Heterocycl. Syst.*, 2004, **8**, 1–32.
7 K. J. McEwan, G. Bourhill, J. M. Robertson and H. L. Anderson, The nonlinear optical characterization of *meso*-substituted porphyrin dyes, *J. Nonlinear Opt. Phys. Mater.*, 2000, **9**, 451–468.
8 S. T. Fu, X. J. Zhu, G. J. Zhou, W. Y. Wong, C. Ye, W. K. Wong and Z. Y. Li, Synthesis, structures and optical power limiting of some transition metal and lanthanide monoporphyrinate complexes containing electron-rich diphenylamino substituents, *Eur. J. Inorg. Chem.*, 2007, 2004–2013.
9 K. Dou, X. D. Sun, X. J. Wang, R. Parkhill, Y. Guo and E. T. Knobbe, Optical limiting and nonlinear absorption of excited states-in metalloporphyrin-doped sol gels, *IEEE J. Quantum Electron.*, 1999, **35**, 1004–1014; C. Y. He, Y. Q. Wu, G. Shi, L. Jiang, W. Duan, Y. Song and Q. Chang, Strong reverse saturable absorptive effect of an ultrathin film containing octacarboxylic cobalt phthalocyanine and polyethylenimine, *J. Porphyrins Phthalocyanines*, 2007, **11**, 496–502.
10 A. Baev, O. Rubio-Pons, F. Gel'mukhanov and H. Agren, Optical limiting properties of zinc- and platinum-based organometallic compounds, *J. Phys. Chem. A*, 2004, **108**, 7406–7416.
11 W. Blau, H. Byrne, W. M. Dennis and J. M. Kelly, Reverse saturable absorption in tetraphenylporphyrins, *Opt. Commun.*, 1985, **56**, 25–29.

12 D. Dini, M. Barthel and M. Hanack, Phthalocyanines as active materials for optical limiting, *Eur. J. Org. Chem.*, 2001, 3759–3769.

13 Y. L. Liu, Z. B. Liu, J. G. Tian, Y. Zhu and J. Y. Zheng, Effects of metallization and bromination on nonlinear optical properties of diphenylporphyrins, *Opt. Commun.*, 2008, **281**, 776–781; Y. Zhu, Y. Z. Zhu, H. B. Song, J. Y. Zheng, Z. B. Liu and J. G. Tian, Synthesis and crystal structure of 21,23-dithiaporphyrins and their nonlinear optical activities, *Tetrahedron Lett.*, 2007, **48**, 5687–5691.

14 M. Zawadzka, J. Wang, W. J. Blau and M. O. Senge, Correlation studies on structurally diverse porphyrin monomers, dimers and trimers and their nonlinear optical responses, *Chem. Phys. Lett.*, 2009, **477**, 330–335.

15 A. Krivokapic, H. L. Anderson, G. Bourhill, R. Ives, S. Clark and K. J. McEwan, *Meso*-tetra-alkynyl porphyrins for optical limiting – A survey of group III and IV metal complexes, *Adv. Mater.*, 2001, **13**, 652–656.

16 P. P. Kiran, N. Srinivas, D. R. Reddy, B. G. Maiya, A. Dharmadhikari, A. S. Sandhu, G. R. Kumar and D. N. Rao, Heavy atom effect on nonlinear absorption and optical limiting characteristics of 5,10,15,20-(tetratolyl) porphyrinato phosphorus(v) dichloride, *Opt. Commun.*, 2002, **202**, 347–352.

17 P. J. Goncalves, L. De Boni, N. M. B. Neto, J. J. Rodrigues, S. C. Zilio and I. E. Borissevitch, Effect of protonation on the photophysical properties of *meso*-tetra(sulfonatophenyl) porphyrin, *Chem. Phys. Lett.*, 2005, **407**, 236–241.

18 F. M. Qureshi, S. J. Martin, X. Long, D. D. C. Bradley, F. Z. Henari, W. J. Blau, E. C. Smith, C. H. Wang, A. K. Kar and H. L. Anderson, Optical limiting properties of a zinc porphyrin polymer and its dimer and monomer model compounds, *Chem. Phys.*, 1998, **231**, 87–94.

19 Y. F. Xu, Z. B. Liu, X. L. Zhang, Y. Wang, J. G. Tian, Y. Huang, Y. F. Ma, X. Y. Zhang and Y. S. Chen, A graphene hybrid material covalently functionalized with porphyrin: synthesis and optical limiting property, *Adv. Mater.*, 2009, **21**, 1275–1279; Z. B. Liu, Y. F. Xu, X. Y. Zhang, X. L. Zhang, Y. S. Chen and J. G. Tian, Porphyrin and fullerene covalently functionalized graphene hybrid materials with large nonlinear optical properties, *J. Phys. Chem. B*, 2009, **113**, 9681–9686.

20 M. O. Senge, C. Ryppa, M. Fazekas, M. Zawadzka and K. Dahms, 5,10-A2B2-Type *meso*-substituted porphyrins-a unique class of porphyrins with a realigned dipole moment, *Chem.–Eur. J.*, 2011, **17**, 13562–13573.

21 E. G. A. Notaras, M. Fazekas, J. J. Doyle, W. J. Blau and M. O. Senge, A(2)B(2)-type push-pull porphyrins as reverse saturable and saturable absorbers, *Chem. Commun.*, 2007, 2166–2168.

22 M. Zawadzka, J. Wang, W. J. Blau and M. O. Senge, Modeling of nonlinear absorption of 5,10-A2B2 porphyrins in the nanosecond regime, *J. Phys. Chem. A*, 2013, **117**, 15–26.

23 *Porphyrins and metalloporphyrins*, ed. K. M. Smith, Elsevier, Amsterdam, Oxford, 1975.

24 K. Sonogashira, Y. Tohda and N. Hagihara, Convenient synthesis of acetylenes – catalytic substitutions of acetylenic hydrogen with bromoalkenes, iodoarenes, and bromopyridines, *Tetrahedron Lett.*, 1975, 4467–4470.

25 E. M. Maya, A. W. Snow, J. S. Shirk, R. G. S. Pong, S. R. Flom and G. L. Roberts, Synthesis, aggregation behavior and nonlinear absorption properties of lead phthalocyanines substituted with siloxane chains, *J. Mater. Chem.*, 2003, **13**, 1603–1613.

26 E. Stulz, C. C. Mak and J. K. M. Sanders, Matrix assisted laser desorption/ionisation (MALDI)-TOF mass spectrometry of supramolecular metalloporphyrin assemblies: a survey, *J. Chem. Soc., Dalton Trans.*, 2001, 604–613; M. J. Crossley, P. Thordarson and R. A. S. Wu, Efficient formation of lipophilic dihydroxotin(iv) porphyrins and bis-porphyrins, *J. Chem. Soc., Perk. Trans. 1*, 2001, 2294–2302.

27 R. J. Abraham, F. Eivazi, H. Pearson and K. M. Smith, Pi-pi aggregation in metalloporphyrins – causative factors, *J. Chem. Soc., Chem. Commun.*, 1976, 699–701; R. J. Abraham, F. Eivazi, H. Pearson and K. M. Smith, Mechanisms of aggregation in metalloporphyrins – demonstration of a mechanistic dichotomy, *J. Chem. Soc., Chem. Commun.*, 1976, 698–699; M. O. Senge, C. W. Eigenbrot, T. D. Brennan, J. Shusta, W. R. Scheidt and K. M. Smith, Aggregation properties of nitroporphyrins: comparisons between solid-state and solution structures, *Inorg. Chem.*, 1993, **32**, 3134–3142.

28 R. F. Pasterna, G. C. Centuro, P. Boyd, L. D. Hinds, P. R. Huber, L. Francesc, P. Fasella, G. Engasser and E. Gibbs, Aggregation of *meso*-substituted water-soluble porphyrins, *J. Am. Chem. Soc.*, 1972, **94**, 4511–4517.

29 L. M. Mink, M. L. Neitzel, L. M. Bellomy, R. E. Falvo, R. K. Boggess, B. T. Trainum and P. Yeaman, Platinum(ii) and platinum(iv) porphyrin complexes: synthesis, characterization, and electrochemistry, *Polyhedron*, 1997, **16**, 2809–2817.

30 S. M. O'Flaherty, S. V. Hold, M. J. Cook, T. Torres, Y. Chen, M. Hanack and W. J. Blau, Molecular engineering of peripherally and axially modified phthalocyanines for optical limiting and nonlinear optics, *Adv. Mater.*, 2003, **15**, 19–32.

31 R. Bonnett, A. Harriman and A. N. Kozyrev, Photophysics of halogenated porphyrins, *J. Chem. Soc., Faraday Trans.*, 1992, **88**, 763–769.

32 K. P. Unnikrishnan, J. Thomas, V. P. N. Nampoori and C. P. G. Vallabhan, Nonlinear absorption in certain metal phthalocyanines at resonant and near resonant wavelengths, *Opt. Commun.*, 2003, **217**, 269–274.

33 J. H. Si, M. Yang, Y. X. Wang, L. Zhang, C. F. Li, D. Y. Wang, S. M. Dong and W. F. Sun, Nonlinear excited-state absorption in cadmium texaphyrin solution, *Appl. Phys. Lett.*, 1994, **64**, 3083–3085; S. N. R. Swatton, K. R. Welford, S. J. Till and J. R. Sambles, Nonlinear absorption of a carbocyanine dye 1,1′,3,3,3′,3′-hexamethylindotricarbocyanine iodine using a Z-scan technique,

Appl. Phys. Lett., 1995, **66**, 1868–1870; P. P. Kiran, D. R. Reddy, B. G. Maiya, A. K. Dharmadhikari, G. R. Kumar and N. R. Desai, Enhanced optical limiting and nonlinear absorption properties of azoarene-appended phosphorus(v) tetratolylporphyrins, *Appl. Opt.*, 2002, **41**, 7631–7636.

34 N. Srinivas, S. V. Rao, D. Rao, B. K. Kimball, M. Nakashima, B. S. Decristofano and D. N. Rao, Wavelength dependent studies of nonlinear absorption in zinc *meso*-tetra(p-methoxyphenyl)tetrabenzoporphyrin (Znmp TBP) using Z-scan technique, *J. Porphyrins Phthalocyanines*, 2001, **5**, 549–554; D. Dini, S. Vagin, M. Hanack, V. Amendola and M. Meneghetti, Nonlinear optical effects related to saturable and reverse saturable absorption by subphthalocyanines at 532 nm, *Chem. Commun.*, 2005, 3796–3798.

35 W. J. Su, T. M. Cooper and M. C. Brant, Investigation of reverse-saturable absorption in brominated porphyrins, *Chem. Mater.*, 1998, **10**, 1212–1213.

36 M. O. Senge, M. Fazekas, M. Pintea, M. Zawadzka and W. J. Blau, 5,15-A(2)B(2)- and 5,15-A(2)BC-Type porphyrins with donor and acceptor groups for use in nonlinear optics and photodynamic therapy, *Eur. J. Org. Chem.*, 2011, 5797–5816.

37 M. O. Senge, Y. M. Shaker, M. Pintea, C. Ryppa, S. S. Hatscher, A. Ryan and Y. Sergeeva, Synthesis of *meso*-substituted ABCD-type porphyrins by functionalization reactions, *Eur. J. Org. Chem.*, 2010, 237–258.

38 M. Sheikbahae, A. A. Said, T. H. Wei, D. J. Hagan and E. W. Vanstryland, Sensitive measurement of optical nonlinearities using a single beam, *IEEE J. Quantum Electron.*, 1990, **26**, 760–769.

